A Peek inside Sensing attachment Techniques of SG Intellectual Property on Electromechanical Charge Density and Waveform Propagation Methods for Diagnostics and Piezo-Impedance Inspection

Venu Gopal Madhav Annamdas (venu.iisc@pmail.ntu.edu.sg)
Dr. Annamdas Venu's Structural Health Lab - Nanyang Technological University, Singapore
John Hock Lye Pang
School of Mechanical and Aerospace Engineering, Nanyang Technological University

Method Article

Keywords: Piezoelectric wafer active sensor (PWAS), Electromechanical admittance (EMA), Impedance, crack, load, permanent, contact, touch, load

Posted Date: June 14th, 2018

DOI: https://doi.org/10.1038/protex.2018.079

Abstract

Piezoelectric wafer active sensor \(PWAS) is an active smart material which is usually attached to the host structure to be monitored. The attached PWAS patch actuates and imports actuations to the host, in presence of electric voltage which then results in unique health diagnostic signal know as electromechanical admittance \(EMA) signature. These EMA signatures change in presence of crack, load or any other degradation in the host structure thus indicating the anomaly. However, the most important drawback of this technique is 'to permanently bond the PWAS to the host structure using adhesive' which destroys the surface aesthetics and makes the location stiff, as a result a weak signature with lower sensitivity will be produced. If large structures are to be monitored then they require several PWAS patches, to be permanently attached, which cannot be reused for any other applications if required. Removing defective PWAS patch at any stage of monitoring also poses a big problem. A provisional patent filed by Nanyang Technological University \(NTU), Singapore \(SG) which was protected between July 2013 to July 2014, discloses several different piezo attachment techniques along with many other implementation schemes suitable for small or large structures. Furthermore, the provisional patent presented two unique structural health monitoring \(SHM) processes using variable electrode based electromechanical charge density \(EMCD) and programmable waveform propagation \(WFP) methodologies. This protocol provides a peek- inside one attachment technique, and its implementation using electromechanical impedance \(EMI). It revolves around a non-contact/ touch PWAS patch, flexibly attached to engineering structure by a magnetic force. However without loss of generality, EMI method instead of EMCD/ WFP method was adopted in the present demonstrations. Some neodymium magnets and contact stress were adopted to generate perfect attachment. Further, a total of four experiments to monitor transverse load, crack, contact stress and axial load were demonstrated. These experiments resulted in successful verification of piezo-magnetic touch sensor for SHM. Contact us for information about other types of stable attachments and EMCD or WFP methods. This work was carried out in the School of Mechanical and Aerospace Engineering \(academic year 2012-13).

Introduction

1.1. Background Last couple of decades had seen a rapid rise in the implementation of smart material \(Reece 2007; Sun et al 2010; Annamdas and Radhika 2013) based structural health monitoring \(SHM). Especially piezoelectric wafer active senor \(PWAS) is one such active smart material which is usually attached by surface bonding or embedding inside the host structure to be monitored for loading, crack or damage \(Park et al 2008; Yan and Chen 2010; Annamdas et al 2013). The attached PWAS patch actuates and imports these actuations to the host, in the presence of electric voltage which then results in unique health diagnostic signal know as electro mechanical admittance \(EMA) signature \(Park et al. 2003). These EMA signatures change in presence of cracks, loads or any other degradation in the host structure thus indicating any existing anomaly. However, the most important drawback of this technique is to permanently bond the PWAS patch to the host structure using adhesive which destroys the surface aesthetics and also makes the location stiff. Furthermore, the bonding layer significantly reduces the

magnitude of the signatures. This especially creates a problem for larger structures as the number of PWAS is usually more \(Madhav and Soh 2007, 2008) and they increase the stiffness of the host structure below the patch. Removing defective PWAS patch at any stage of monitoring also poses a big problem. Furthermore after monitoring period is over, they cannot be reused elsewhere even if the PWAS patch is in good condition. This protocol thus presents potential applications of touch PWAS patch, which stay in contact with the host structure by a reasonable force \(to ensure interaction between patch-host), imports the actuations to the host to generate health signature as similar to bonded/ embedded PWAS patch. This reasonable force is provided by neodymium magnets in the first, second and fourth experiments, and by contact stress in the third experiment. Experiments 1, 2 and 3 were performed to monitor transverse load, crack, and contact stress respectively for boundary conditions of simply support, fixed-fixed and simply support ends of the same aluminium beam, whereas the experiment 4 was performed to monitor axial load for fixed-fixed boundary condition of a laser clad steel specimen. Thus, a total of four experiments resulted in successful verification of touch sensor on aluminium and steel specimens for EMA based SHM. 1.2. The Electromechanical Admittance \(EMA) technique The EMA technique is one of popular developments in the field of smart material based SHM. In the EMA technique, the governing principle is that a PWAS is permanently bonded to the host structure via a layer of epoxy adhesive \(Madhav and Soh 2007), this PWAS actuates harmonically at high frequencies \(< 500 kHz) in the presence of electric field. These actuations are transferred or imported to the host structure via the bonding layer \(and subsequent shear lag effect) to produce a structural response which is EMA signature. This EMA signature is a function of the stiffness, mass and damping of the host structure \(Sun et al. 1995), length, width, thickness, orientation and mass of the PWAS patches \(Madhav and Soh 2008) and thickness of bonding layer \(Madhav and Soh 2007). The changes in the EMA signature, which is the inverse measure of mechanical impedance of the structure, are indicative of the presence of structural anomaly. However in the recent past, researchers \(Na et al 2013; Tawie et al 2013) are working to develop re-usable PWAS either as magnetic-reusable sensor, or nut-bolt sensor or embedded-reusable sensor \(Yang et al 2010). In these cases, the interaction between the PWAS and the structure is not direct but via a medium \(such as magnet or bolt or epoxy layer or casing etc). In the past it was studied that the \(Madhav and Soh 2007) thickness of the bonding epoxy layer influences the admittance signatures to a great extent. Hence there is need to develop not just a reusable PWAS patch but also to develop a successful interaction mechanism between patch and the host as demonstrated in Figure 1. Figure 1\(a) shows latest magnetic-PWAS patch devised by Na et al \(2012), Figure 1\(b) shows a proposed bonding layer free but magnetic force supported PWAS patch used in experiments 1, 2 and 4, and Figure 1\(c) shows the proposed bonding layer free but contact force supported touch sensor used in experiment 3. Thus touch sensors were used for monitoring non-ferromagnetic aluminium specimen in the first three experiments and ferromagnetic steel specimen in the fourth experiment. 1.3. Piezoelectric Wafer Active Sensor \(PWAS) patches PWAS patches are usually in the shape of circle or square \(Yang et al 2008; Lim and Soh 2012, 2014). The PWAS patch, which can be directly connected to an electrical analyzer, such as the Agilent's LCR \(inductance -L, capacitance -C, and resistance -R measuring) meter \(Agilent 2014) is as shown in Figure 2\(a) and experimental specimens are as shown in Figures 2\(b-f). The LCR meter imposes an alternative voltage signal of 1 volt rms to the attached PWAS patch over the

user specified frequency range. The changes in extracted admittance signature are indicative of the presence of structural loading changes or boundary changes \(Annamdas et al 2007) or damages \(Park et al 2003). In principle, the EMA based SHM technique is similar to the conventional global vibration techniques. The major difference is only with respect to the frequency range employed, which is typically <500 kHz for this techniques against less than 100 Hz for the global vibration techniques. The peaks are proportional to the natural frequencies of the host structure and shifting of these peaks indicate changes in the natural frequencies of the structure which can arise due to crack/ load in the structure \(Park et al 2003; Annamdas et al 2014). The technique has several advantages over the conventional damage or load measurement based techniques. It employs low-cost and low-power PWAS patches, which can be non-intrusively bonded to the structure and can be interrogated without removal of finishes.

Equipment

\(1) LCR meter for acquiring admittance signature consists of an \(Figure 2a), controlled by a personal computer was connected to Aluminium and Steel specimens \(Table 1). \(2) Specimens and the locations of PWAS patches are as shown in Figure 2. Experiments 1, 2 and 3 were performed to monitor transverse load, crack, and contact stress respectively for boundary conditions of 'simply support', 'fixed-fixed' and 'simply support' ends of an aluminium beam whereas the experiment 4 was performed to monitor axial load for 'fixed-fixed' boundary condition of a laser clad steel specimen. \(3) An aluminium beam \[A1 6061-T6], placed on two simply supports as shown in Figure 2\(b-c) \(details of experiment 1). \(A) One PWAS patch \(say PWAS-p), permanently bonded at 9 cm away from one edge whereas another PWAS patch \(say PWAS-t), placed at 9 cm away from the other edge. \(B) A round circular Neodymium magnet of 12 mm diameter and 4 mm thickness was simply placed on the magnet \(designated as main magnet shown in Figure 2\(b)). \(C) A support magnet was attached, exactly below the main magnet on other side as shown in Figure 2\(c). As the specimen is aluminium \(a non ferro-magnetic) and hence two magnets are required to provide the necessary force to attach the PWAS-t patch to the specimen. \(D) Both these PWAS-p and PWAS-t patches are connected to the same LCR meter for signature acquisition. \(4) An AISI steel of grade 4320 \(Steel 2014) specimen with 1 mm thick laser clad layers on the central location on both sides of the specimen. \(5) A 10 ton Endurance Testing System of Shimadzu \[2014] was adopted,

Procedure

2.1 Experimental Investigations and Discussion All the experiments are repeatable, readers can follow the procedures outlined to replicate our results. -- Procedure for the strip \(transverse) load monitoring \(experiment 1), \(A) Place a hanger \(of 100 gm weight) of 1 cm wide at the centre as shown in Figure 2\(c). \(B) Increase loads/ weights in steps from 100 gm until 1500 gm in steps of 200 gm by hanging them to the hanger. \(C) At each load state of the specimen, two readings were acquired from the LCR meter \(by two patches) for a frequency range of 10 to 150 KHz at sweep steps of 0.25 KHz. \(D) Obtain readings at baseline \(healthy state) before placing the hanger \(i.e at 0 gm), after attaching hanger at

centre \(i.e at 100 gm), later at every load increment of 200 gms. \(E) Your obtained signatures from the PWAS-p patch can resemble Figure 3. In experiment 1, a clear distinction between conductuance and suceptance signatures existed. The signatures contain several distinct peaks, which either shifted towards right/ left \(indicating increase/ decrease in frequency) or deviated upward/ downward \(indicating an increase/ decrease in magnitude of admittance). \(F) If a peak shift to right than some other peak shifts left or vice versa and thus in general all such features are common when structure is subjected to the loading \(Annamdas et al 2007). \(G) A careful inspection, which is termed as signature analysis \(Annamdas et al 2014) should be carried out at representative tall peaks such as 1, 2 ,3 and 4 \(as indicated in the Figure 3) in Figure 4 \(a-b-c-d). 2.2 Key features of signatures \(for permanent PWAS patch) \(A) Obtain baseline signature before placing hanger on the beam and note that the hanger placement slightly displaces the boundary condition. \(B) Obtain loaded signatures, there will not be boundary disturbances during loading. Figure 4\(a) shows signatures in the frequency range of 27-29 KHz, which presents some peaks that shifted upwards whereas the peak at 28.25KHz, indicated as 1, did not show any consistent shifting. Thus, taller peak need not show any trend of increase or decrease as load increased on the specimen. Figures 4 \(b - c) shows peaks at 85.75 KHz and 121 KHz respectively, which presented a decreasing and an increasing trend as the load magnitude on the beam increased. Figure 4\(d) shows a frequency range where both downward and upward shifting of different peaks were observed. Thus, the characteristic features of signatures for loaded specimen comprises of several peaks which either increase or decrease in magnitude as load increased. Hence a touch sensor also should retain these key features. 2.3 Key features of signatures \(for the touch sensor) \(A) Obtain signatures for 0 gm to 1500 gm load on the specimen at all load increments using PWAS-t patch. Your signatures can resemble Figure 5. Unlike PWAS-p, these can result in the larger magnitudes which can be added advantage. As it means that PWAS - t is more sensitive compared to permanently bonded PWAS-p patch due to absence of any bonding layer. \(B) Obtain a close-up view at various locations as it can show variations clearly, as similar to close-up view of Figures 6 \(a-d). This type of signature analysis helps to find out the characteristic features of touch sensor. \(C) Do comparative study. In our case, Figure 6\(a) shows a peak at 28.25 KHz, which is neither increasing nor decreasing as similar to Figure 4\(a) of PWAS-p patch. Furthermore zero-loaded signature is different from loaded signatures indicating a probable change in boundary conditions, and this shift is more obvious compared to Figure 4\(a). \(D) Touch sensor can show difference in boundary condition of specimen for 0gm and subsequent loads, more obviously than the permanent patch. Figure 6\(b) shows some peaks in the range of 85.5 to 87 KHz, which shifted either upward or downward or without clear trend, i.e the behaviour is similar to PWAS-p \(Figure 4b) but the direction of shifting is different. \(E) Observe any interesting features in frequency domain. In our case, there existed larger peaks beyond 86KHz \(see Figure 5) and thus two frequency ranges were closely observed as shown in Figure 6\(c-d), to see if anything interesting can be obtained. Figure 6 \(d) shows a very sensitive range where the peaks shifted in higher magnitudes, than Figure 6\(c), which too show the upward or downward deviations of loaded specimen. \(F) Observe any interesting features such as change in boundary conditions. In our case, two boundary conditions i.e at baseline \(0 gm) and at loading process were observed. These signatures \(Figure 6: a-d) show lots of information which is similar or better than the information provided by PWAS-p \(Figure 4: a-d), which is so far

considered to be best in SHM applications for EMA. It should be noted that the interaction between PWAS-p and host structure is by an epoxy layer \(Madhav and Soh 2007), whereas in this PWAS-t, epoxy adhesive is absent and the interaction between patch and host structure is direct. However, there will not be any structural peaks but the magnetic force provides a unique bonding force. At least in our experiment, the sensitivity of this PWAS-t patch seems to be better. \(Note: Selection of magnet plays important role.) 2.4 Incremental crack effect on signatures obtained from PWAS-p and PWAS-t – Procedure for the crack monitoring \(experiment 2 is shown in Figure 2\(d), it was a specimen with fixed-fixed boundary condition). Readers can replicate our results as follows. \(A) Induce cracks of 1 cm at some locations starting from PWAS-t. \(B) Record signatures from both patches after inducing cracks \(at 0 cm, 3 cm, 6 cm, 9 cm, 12 cm, 15 cm, 18 cm and 21 cm) at regular intervals, away from the PWAS-t patch as shown in Figure. Experiment2 resulted in signatures which presents larger magnitude shifts unlike the loading increment case. See Figures 7 and 8, signatures obtained from both PWAS-p and PWAS-t at all crack increments, \(c) Readers can use sharp blade to induce cracks on specimen but in our experiment, we used hacksaw blade. This created much disturbance to the structure and it got reflected as 'high magnitude changes in peaks and valleys'. It should be noted that the crack magnitude increased in steps from the location of PWAS-t towards PWAS-p as shown in Figure 2\(d). \(D) You can obtain 2 sets of signatures, when cracks are induced away from PWAS-t and approaching PWAS-p. \(E) The signatures shift so large that the 'signature analysis' as carried-out in the previous load increment case cannot be appropriate because it does not provide meaningful shifting patterns of peaks. \(F) Apply root mean square deviation \(RMSD) index to study the deviations, especially to quantify changes in signatures \(Park et al 2006, Annamdas and Yang 2012). The RMSD is a comparable index of the initial signature with later stage signatures \(k = 1, 2,3 …). In the present study the RMSD index was adopted to evaluate the signatures obtained from the ‘PWAS-specimen’ system. \(G) Tabulate your results. Table 2-columns 2 and 3, presents the RMSD values obtained for crack increments as listed in column 1. \(H) Observe any interesting trends. RMSD indices obtained from PWAS-p shows increasing trends as the crack magnitudes increased towards its direction whereas the RMSD indices obtained from PWAS-t shows decreasing trends as the cracks increased in the opposite direction. The larger magnitudes of RMSD indices of PWAS-t compared to RMSD-p is attributed to direct interaction between PWAS-t and the host structure unlike PWAS-p \(which is via bonding layer). This also depends on magnetic force magnitude. \(I) The larger values also can be attributed to the movement of main and support magnets during the cracking process by hacksaw blade. \(J) In real applications the cracks are seldom generated using a hacksaw blade but they occur due to natural process and hence the movement of magnets will not occur. From experiments 1 and 2 \(load and crack increment studies) it is understood that PWAS-t is effective in dealing with SHM applications on par or better than PWAS-p. Experiments 3 and 4 were thus carried out with only PWAS-t for aluminium and steel specimens respectively as follows. 2.5 Contact load monitoring by PWAS-t – Procedure for the Contact load monitoring \(experiment 3 is shown in Figures 1\(c) and 2\(e), it was a specimen with is simply supported boundary condition as similar to experiment 1). Readers can replicate our results as follows. \(A) Place a PWAS patch on the centre of the specimen without bonding. \(B) Record a baseline signature. \(C) Place a load of 200 gm at the centre such that a part of the load is applied on the sensor and the rest encircling the patch as shown in figures. \(D) Record

the signature, again in load condition. \(E) Place more weights of 200 gm on the top of the existing weight \(F) Record the signature for each load increment. \(G) Plot all the signatures. Figure 9\(a) shows these signatures for all load magnitudes in our experiment. \(H) Now, carried-out unloading systematically by removing each load and obtain subsequent signature. Plot them as similar to Figure 9\(b). \(I) Do a careful signature analysis to compare between loading and unloading processes: Our analysis reveals that there exists rightward shifting during loading and leftward shifting of peaks during unloading. \(J) Apply RMSD index to study the difference of loading and unloading, as listed in columns 5 and 6, at load magnitudes as listed in column 4 of Table 2. \(K) Obtain any interesting facts from RMSD table: From Table2, an interesting observation was obtained, i.e a total load of 600-800 gm seems to be optimal to get a estimation of over 100 % increase in RMSD values, where as any further increment of load decreases the RMSD values \(indicating a decrease in sensitivity). During loading or unloading process, the optimal load to be placed to obtain effective interaction between patch and the structure is anywhere between 600-800 gm. More specifically, it is 3.14/16 times the total load \(see Figure 2e) on the PWAS-t patch. \(L) Touch sensor characterization: our study demonstrates that touch sensor can operate if a pre-requisite force is placed on the patch even without any magnetic force. However, if more force is applied on the patch, it reduces the RMSD \(Table 2) and is ineffective. \(M) Make a comparison between this and other previous experiments. For example, the magnitudes of signatures and the RMSD values were larger in experiments 1 and 2 when magnetic force was used than the permanently bonded patch. \(N) Make a detailed study about magnetic force effect on signature. It should not be misunderstood that heavier magnets or heavier loads on the patch can give larger magnitude signatures or larger RMSD indices always. Thus, a study to optimize 'requisite force' to hold the touch sensor on the structure is necessary before applying them to any SHM application as carried out in this experiment. This requisite force can be considered as alternate to the bonding layer. Any shear lag \(Madhav and Soh 2007) between the patch and the host can be effectively avoided. 2.6 Axial-tensile load monitoring by PWAS-t – Procedure for the Axial-tensile load monitoring \(experiment 4 is shown in Figure 2\(f). Only one magnet to hold the touch sensor on the laser clad steel specimen was adopted unlike experiments 1 and 2). Readers can replicate our results as follows. \(A) Select any specimen suitable for to monitor axial - tensile load such as an “AISI steel of grade 4320 \(Steel 2014) specimen” with 1 mm thick laser clad layers on the central location on both sides of the specimen. \(B) Mount the specimen on Endurance Testing System. \(C) Use fixed- fixed boundary conditions. \(D) Obtain a baseline signature at the healthy state of the specimen for frequency range such as 10 to 200 KHz. \(E) Increase tensile load \(or stress) in steps and record subsequent signatures. \(F) Plot signatures obtained during the tensile test as similar to Figure 10. Plot presents a very reasonable shifting of peaks and valleys during the process of loading. \(G) Apply RMSD index to study the changes in the signatures during loading compared to baseline signature. Indices of present experiment are listed in column 8 of Table 2 for load magnitudes as listed in column 7. The RMSD indices increased gradually as the tensile load increased on the laser clad steel specimen

Anticipated Results

This protocol presented four experiments, which demonstrated the effectiveness of the touch sensor. In experiment 1, two magnets were used to hold the PWAS patch on to the aluminium structure. A load increment study was systematically carried out and signature analysis was performed to understand the features of EMA signature. The touch sensor produced all characteristic features such as peaks shifting upwards or downwards, which is similar to any other permanently bonded PWAS patch. Furthermore, the absence of bonding layer improved the interaction between the patch and the structure, hence it resulted in larger magnitude signatures compared to permanently bonded patch. In experiment 2, crack increment study was carried out. The signature analysis is not relevant for this experiment as the signatures shifted drastically and thus RMSD was used to understand the behaviour of the crack increments. Even in this experiment, PWAS-t resulted in greater magnitudes of peaks as well as larger RMSD values. Thus from both experiments, the PWAS-t patch was found to be suitable for SHM application and hence this sensor was alone used in the experiments 3 and 4. This experiment was carried out to find the optimal load to be placed on the touch sensor for SHM applications. A larger load on the patch decreases the RMSD values and thus reduces the sensitivity. Hence it cannot be mistaken that a heavier or powerful magnet can result in larger magnitude signatures and an optimal study has to be always performed. In the final experiment axial -tensile load was monitored successfully on a laser clad steel specimen using only one magnet to hold the touch sensor effectively. Thus experiments 1 and 4 successfully presented 'transverse and axial load' monitoring respectively for aluminium material and steel material using magnetic force. Experiment 2 presented crack monitoring where as experiment 3 presented force requirement study for a touch sensor during contact stress monitoring. All these four experiments effectively validated the touch sensor. This shows that any major experiments can be performed using the touch sensor for load monitoring or crack monitoring. Figure 11 shows a letter related to SG Intellectual Property, which was protected in SG from Date of issue for a period of one year. At present, there is no more protection on it but we still would not disclose its contents. However interested parties/ labs can contact correspondence author for more information related to other flexible/ reliable attachments, electromechanical charge density \(EMCD) and programmable wave form propagation \(WFP) methodologies. Details related to IP submission and acknowledgement letters are available in "link":http://data.mendeley.com/datasets/gbn4pzrvzs/1 Readers can also look for traditional methods of piezo attachments to host structures such as surface bonding by glue and embedment, in the following review article. Annamdas V. G. M and Radhika M. A \(2013) "Electromechanical Impedance of Piezoelectric Transducers for Monitoring Metallic and Non Metallic Structures: A review of Wired, Wireless and Energy Harvesting Methods" Journal of Intelligent Material Systems and Structures, Volume 24, Issue 9, June 2013 pp. 1019 - 1040 "link":https://doi.org/10.1177/1045389X13481254 Readers can also go through the following article, which demonstrates piezo's surface bonded type of attachment for monitoring fatigue defects and its comparisons to digital image correlation \(DIC) method. Annamdas V. G. M, Chew Y , Pang J. H. L , Hoh H. J, Zhou K and Song B \(2014) "Fatigue growth analysis of interacting and merging surface defects using PZT transducer based impedance method and digital image correlation system.", Journal of Nondestructive Evaluation, Volume 33\(3), pp 413-426, DOI: 10.1007/s10921-014-0237-9. Publisher: Springer US. "link":https://doi.org/10.1007/s10921-014-0237-9 Notes: 1. Consider this protocol as Datasheet/ Supplementary content or Sneak a peek inside a SG

Intellectual Property. It demonstrated the importance of attachments in one type of SHM method but this Piezo - Magnetic touch sensor and its attachment can be applied even for EMCD and WFP methods. 2. The demonstrations related to protocol, patent and its associated journal articles were carried out in School of Mechanical and Aerospace Engineering \(academic year 2012-13), Nanyang Technological University - Singapore.

References

1.Agilent " E4980A Precision LCR Meter" http://www.home.agilent.com/en/pd-715495-pn-E4980A/precision-lcr-meter-20-hz-to-2-mhz?&cc=SG&lc=eng \(2014) 2. Annamdas V. G. M, Yang Y and Soh C. K "Influence of loading on the electromechanical admittance of piezoceramic transducers", Smart Materials and Structures, 16\(5): 1888-1897\(2007) 3.Annamdas V. G. M and Yang Y " Practical implementation of piezo-impedance sensors in monitoring of excavation support structures " Structural Control Health Monitoring, 19\(2) 231–245 \(2012) 4.Annamdas V. G. M and Radhika M. A "Electromechanical Impedance of Piezoelectric Transducers for Monitoring Metallic and Non Metallic Structures: A review of Wired, Wireless and Energy Harvesting Methods", Journal of Intelligent Material Systems and Structures, 24\(9) 1019 - 1040 \(2013) 5.Annamdas V. G. M, Pang J. H. L, Zhou K and Song B "Efficiency of Electromechanical Impedance for Load and Damage Assessment along Thickness of PZT Transducers in Structural Monitoring" Journal of Intelligent Material systems and structures 24\(16) 2008-2022 doi:10.1177/1045389X13488252 \(2013) 6.Annamdas V. G. M, Lim S .I, Pang J. H. L and Soh C. K "Monitoring of fatigue in welded beams using piezoelectric transducer based impedance technique", Journal of Non destructive Evaluation, 33\(1)124-140, DOI:10.1007/s10921-013-0209-5 \(2014) 7. Lim Y Y and Soh C KEffect of varying axial load under fixed boundary condition on admittance signatures of electromechanical impedance technique Journal of Intelligent Material Systems and Structures 1045389X12437888, first published on March 15, 2012 doi:10.1177/1045389X12437888 \(2012) 8.Lim Y Y and Soh C K Electro-Mechanical Impedance \(EMI)-Based Incipient Crack Monitoring and Critical Crack Identification of Beam Structures, Research in Nondestructive Evaluation 25 \(2), 82-98 \(2014) 9.Madhav A. V. G and Soh C. K "Electromechanical Impedance Model of Piezoceramic Transducer - Structure in Presence of Thick Adhesive Bonding", Smart Materials and Structures 16\(3): 673-686 \(2007) 10.Madhav A. V. G and Soh C. K " Uniplexing and Multiplexing of PZT Transducers for Structural Health Monitoring", Journal of Intelligent Material systems and structures 19\(4): 457-467 \(2008) 11.Na, S., Tawie, R., and Lee, H.K. “Electro-mechanical impedance method of fiber-reinforced plastic adhesive joints in corrosive environment using a reusable piezoelectric device,” Journal of Intelligent Material Systems & Structures, 23\(7), 737-747 \(2012). 12.Park, G., Sohn, H., Farrar, C.R. and Inman, D.J. “Overview of Piezoelectric Impedance-Based Health Monitoring and Path Forward.” The Shock and Vibration Digest, SAGE Publications, 35:451-463. \(2003). 13.Park, S., Ahmad, S., Yun, C. B., and Roh, Y.. “Multiple Crack Detection of Concrete Structures Using Impedance-based Structural Health Monitoring Techniques”, Experimental Mechanics, 46\(5) 609-618 \(2006) 14.Park, S., Yun, C.-B. and Inman, D. J. Structural health monitoring using electro-mechanical impedance sensors. Fatigue & Fracture of Engineering Materials & Structures, 31: 714–724. doi: 10.1111/j.1460-2695.2008.01248.x \(2008)

15.Reece P L. Smart Materials and Structures: New Research, Nova Science Publishers., \(2007) 16.Shimadzu "Fatigue and Endurance Testing System of Shimadzu, http://www.shimadzu.ru/brochures/C225-E020_Servopulser_General.pdf \(2012) 17.Steel http://www.steelexpress.co.uk/aisi-sae.html \(2014) 18.Sun M, Staszewski W. J, and Swamy R. N., “Smart Sensing Technologies for Structural Health Monitoring of Civil Engineering Structures,” Advances in Civil Engineering, 2010, Article ID 724962, 13 pages, doi:10.1155/2010/724962 \(2010) 19.Tawie R, Na S and Lee H K " A study of reusable electromechanical impedance methods for structural health monitoring of civil structures ", Proc. SPIE 8692, Sensors and Smart Structures Technologies for Civil, Mechanical, and Aerospace Systems 2013, 869235 \(April 19, 2013); doi:10.1117/12.2010077;http://dx.doi.org/10.1117/12.2010077 \(2013) 20.Yan W and Chen W. Q., “Structural Health Monitoring Using High-Frequency Electromechanical Impedance Signatures,” Advances in Civil Engineering, vol. 2010, Article ID 429148, 11 pages, doi:10.1155/2010/429148 \(2010) 21.Yang, Y. and Divsholi, B. S. " Sub-Frequency Interval Approach in Electromechanical Impedance Technique for Concrete Structure Health Monitoring", Sensors, 10:11644-11661 \(2010)

Acknowledgements

Inventors of SG Intellectual Property \(and authors of this protocol) would like to thank Radhika Madhav Annamdas and Shantanu Vasudev Krishna Annamdas. They advised us to articulate a simple attachment technique and their applications for SHM so that it helps readers to peak inside SG Intellectual Property of Nanyang Technological University \(NTU), Singapore \(SG) and will raise their curiosity to know more attachments. Authors would also like to thank Prof Soh Chee Kiong, School of Civil and Env. Engineering for his encouragement throughout period of invention, NTU.

Figures

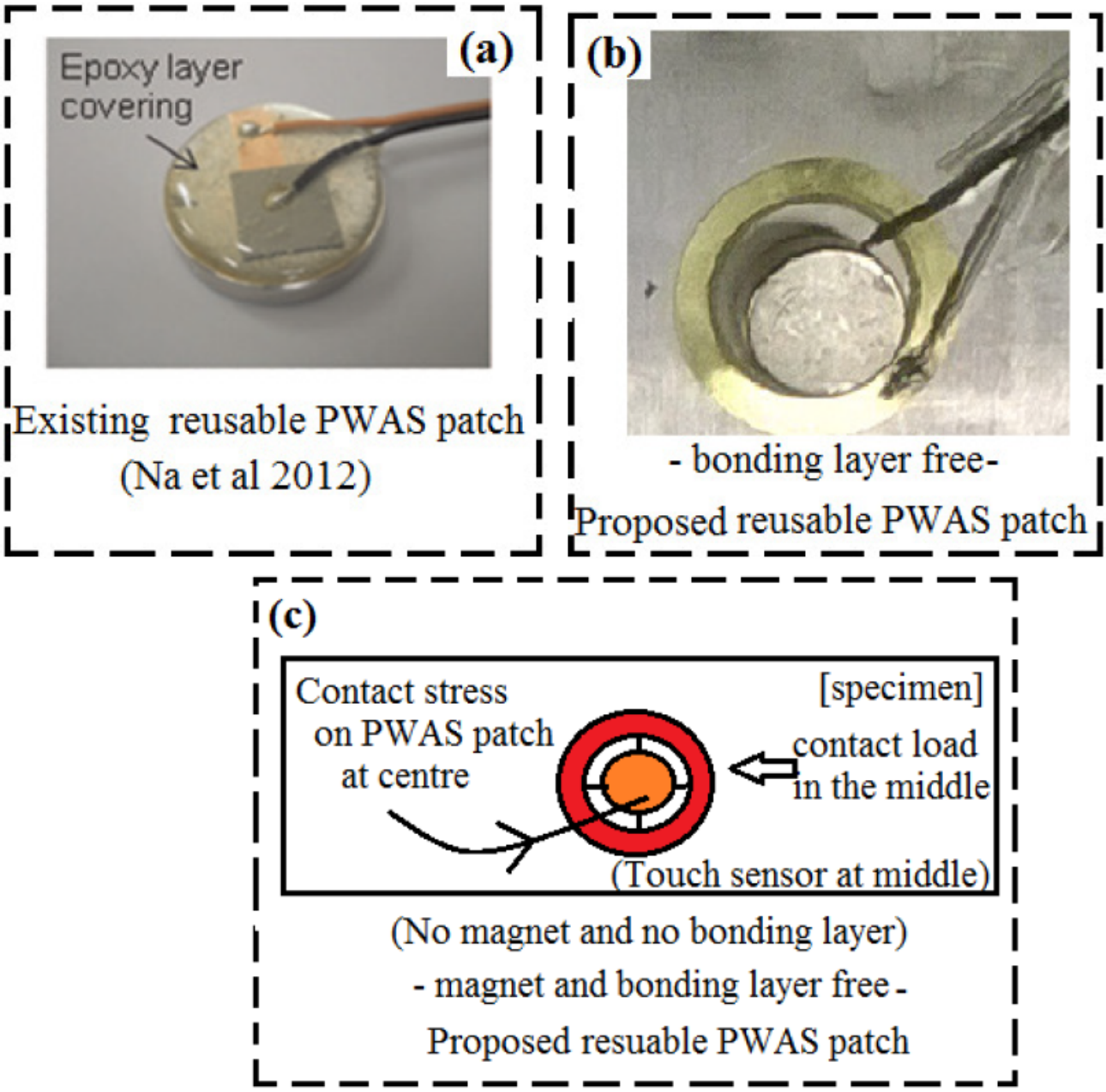

Figure 1. Reusable PWAS (a) existing patch (b) proposed patch for experiments 1 and 2 (c) proposed patch for experiment 3

Figure 1

Reusable PWAS

Figure 2

Experimental Details

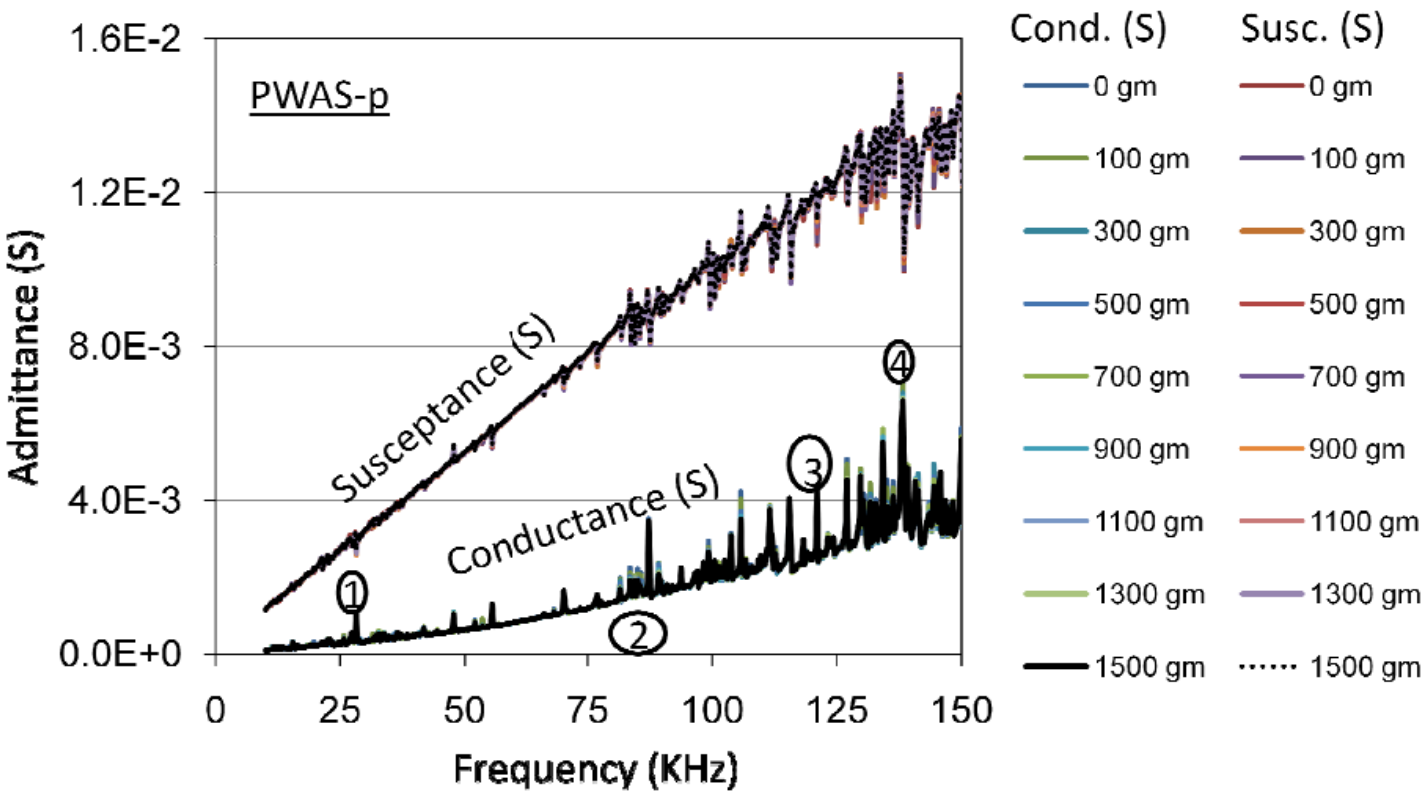

Figure 3. Experimental admittance versus frequency spectrum obtained by permanent PWAS-p patch

Figure 3

Admittance - permanent PWAS-p

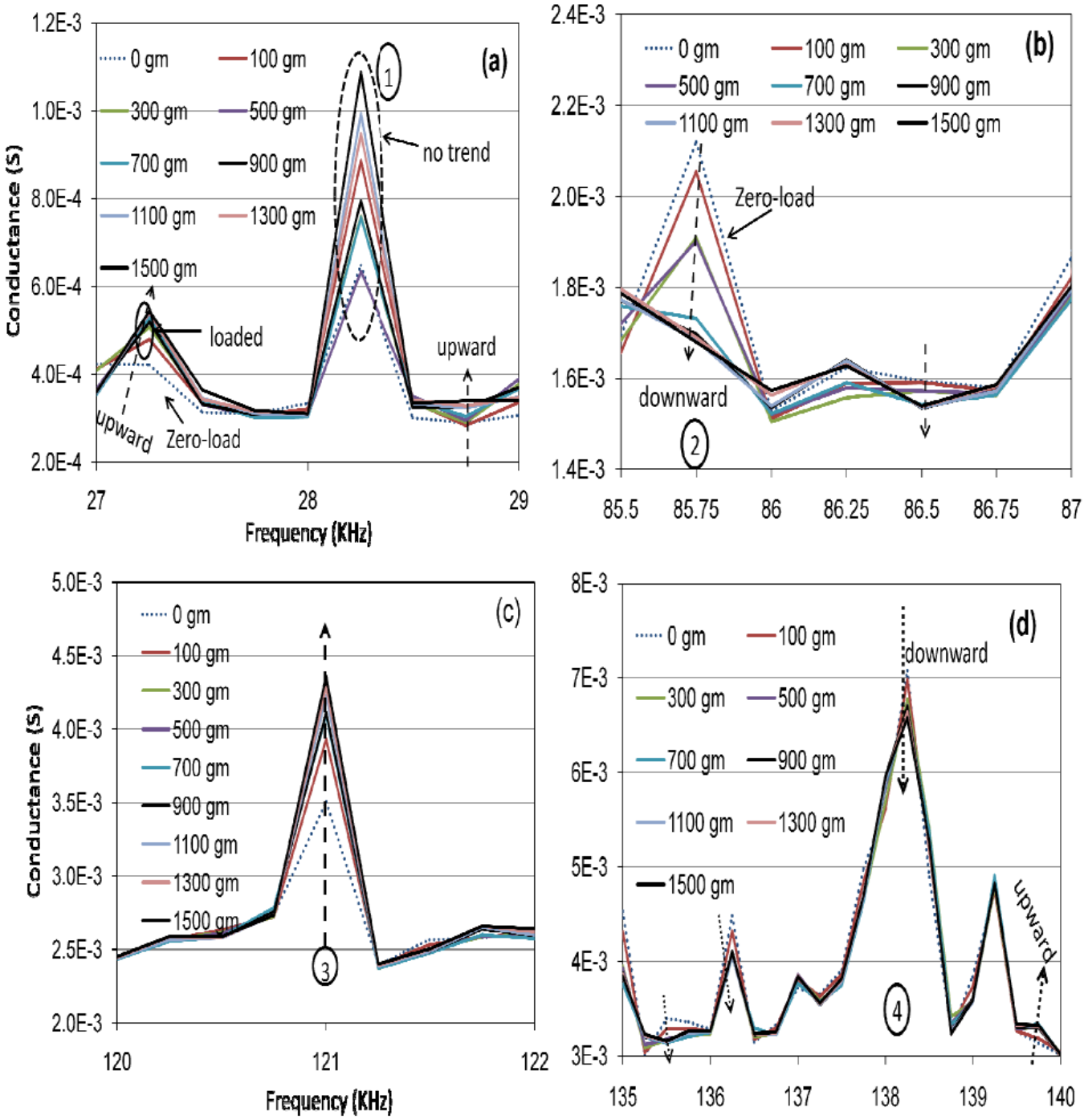

Figure 4. Signature analysis at few prominent peaks and their behaviour (a) no trend at major peak (b) downward trend (c) upward trend (d) both upward and downward trends

Figure 4

Signal Analysis of Prominent Peaks

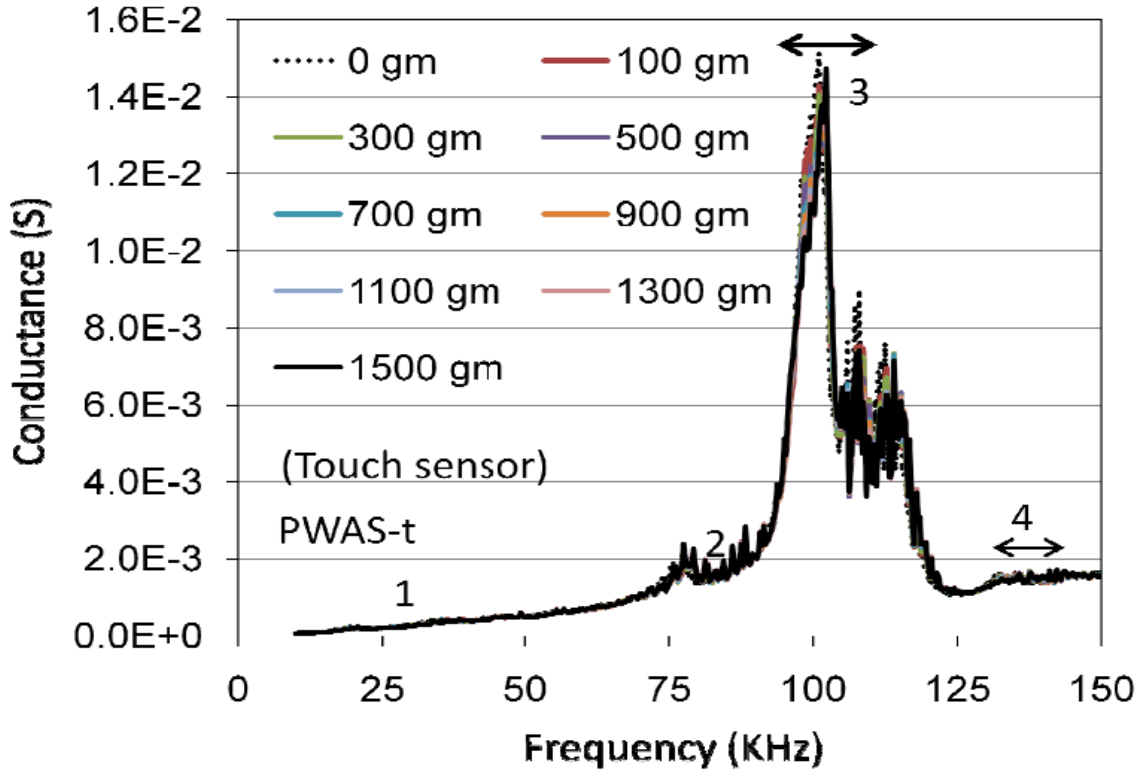

Figure 5. Experimental admittance versus frequency spectrum obtained by reusable and touch PWAS-t patch

Figure 5

Signal Analysis of Prominent Peaks (reusable patch)

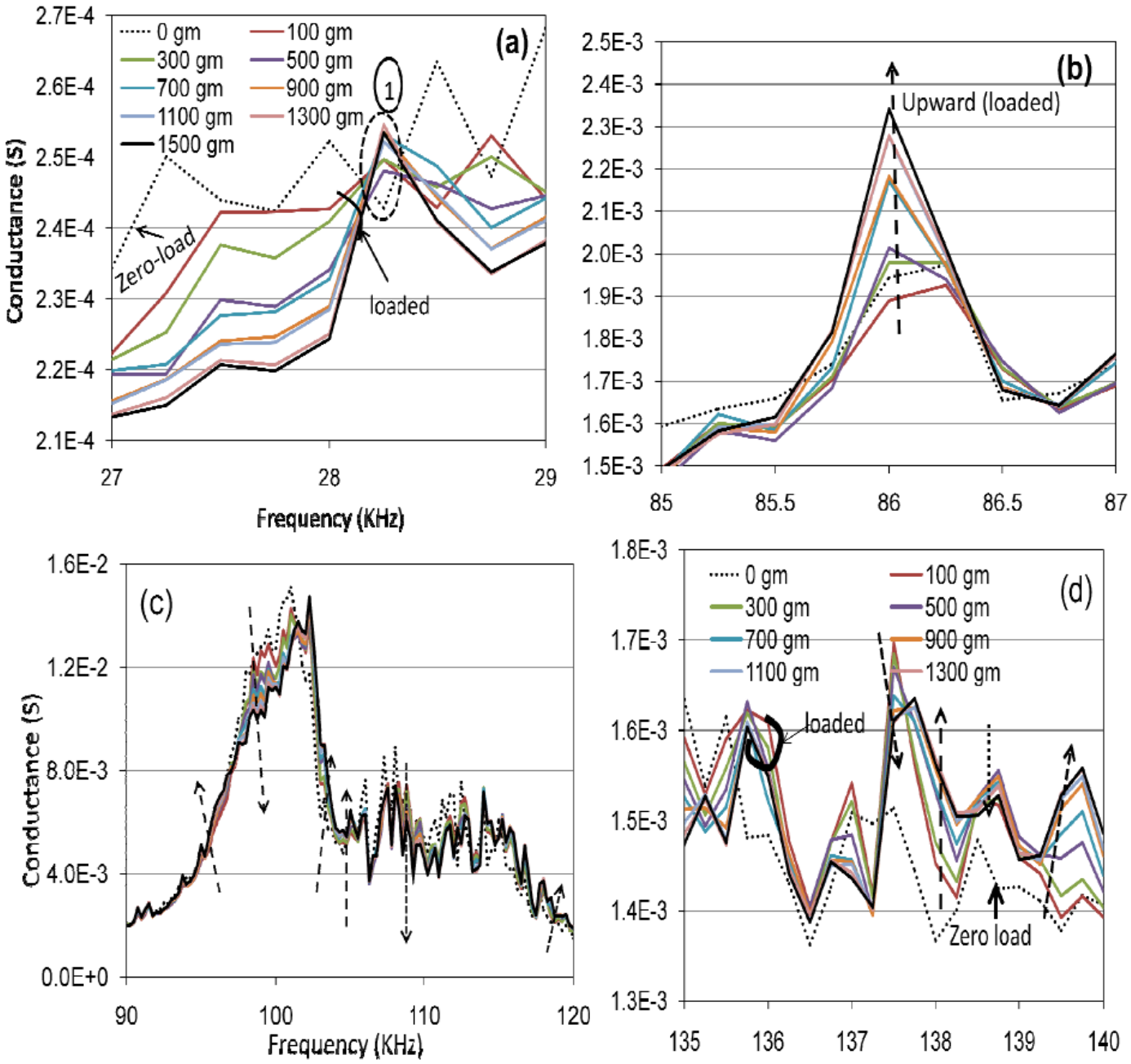

Figure 6. Signature analysis at few prominent peaks and their behaviour (a) no trend at major peak (b) downward trend (c) upward trend (d) both upward and downward trends

Figure 6

Signal Analysis of Prominent Peaks

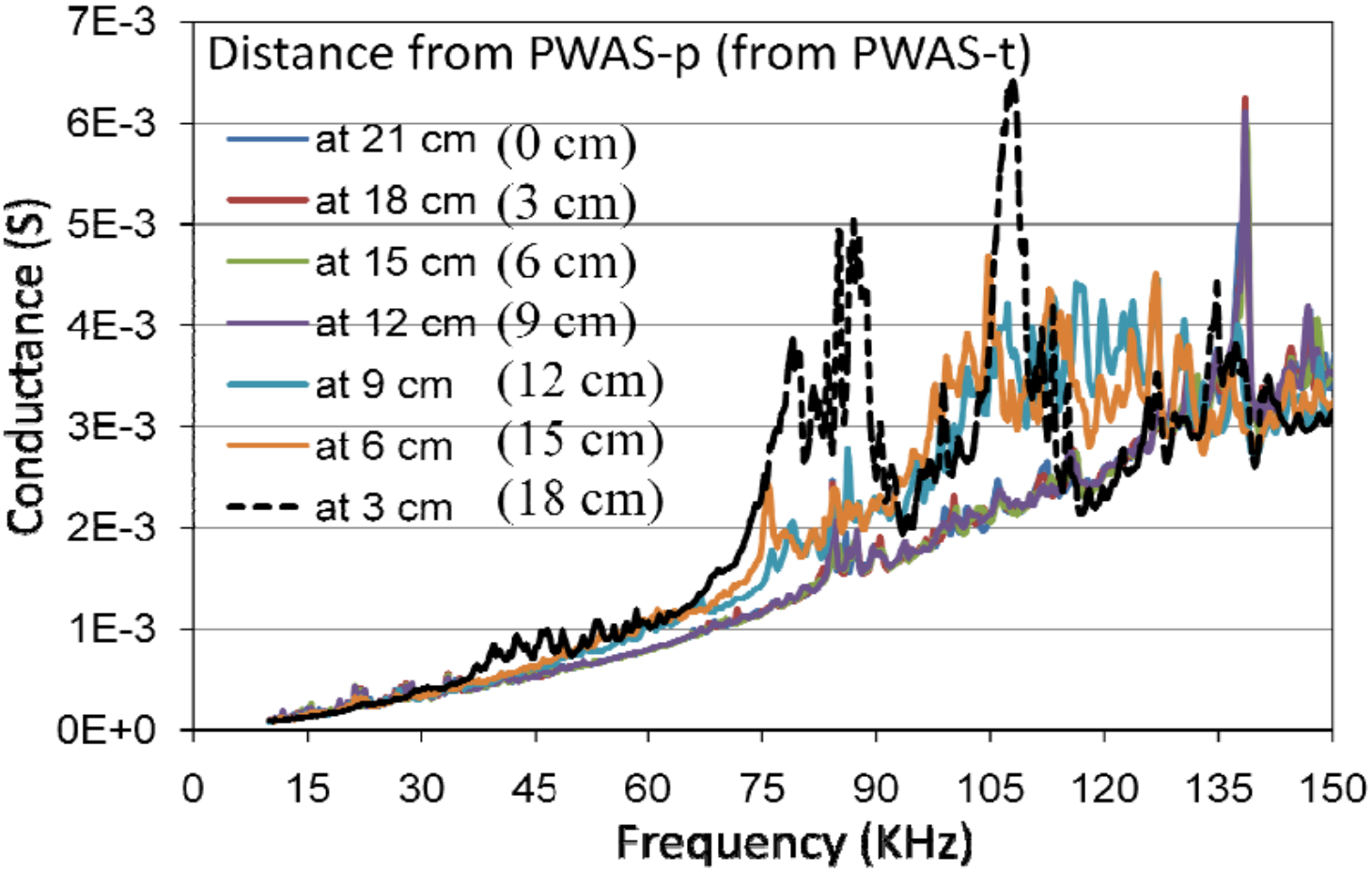

Figure 7. Signatures of crack increments obtained by PWAS-P

Figure 7

Signal Analysis of crack increments (PWAS-p)

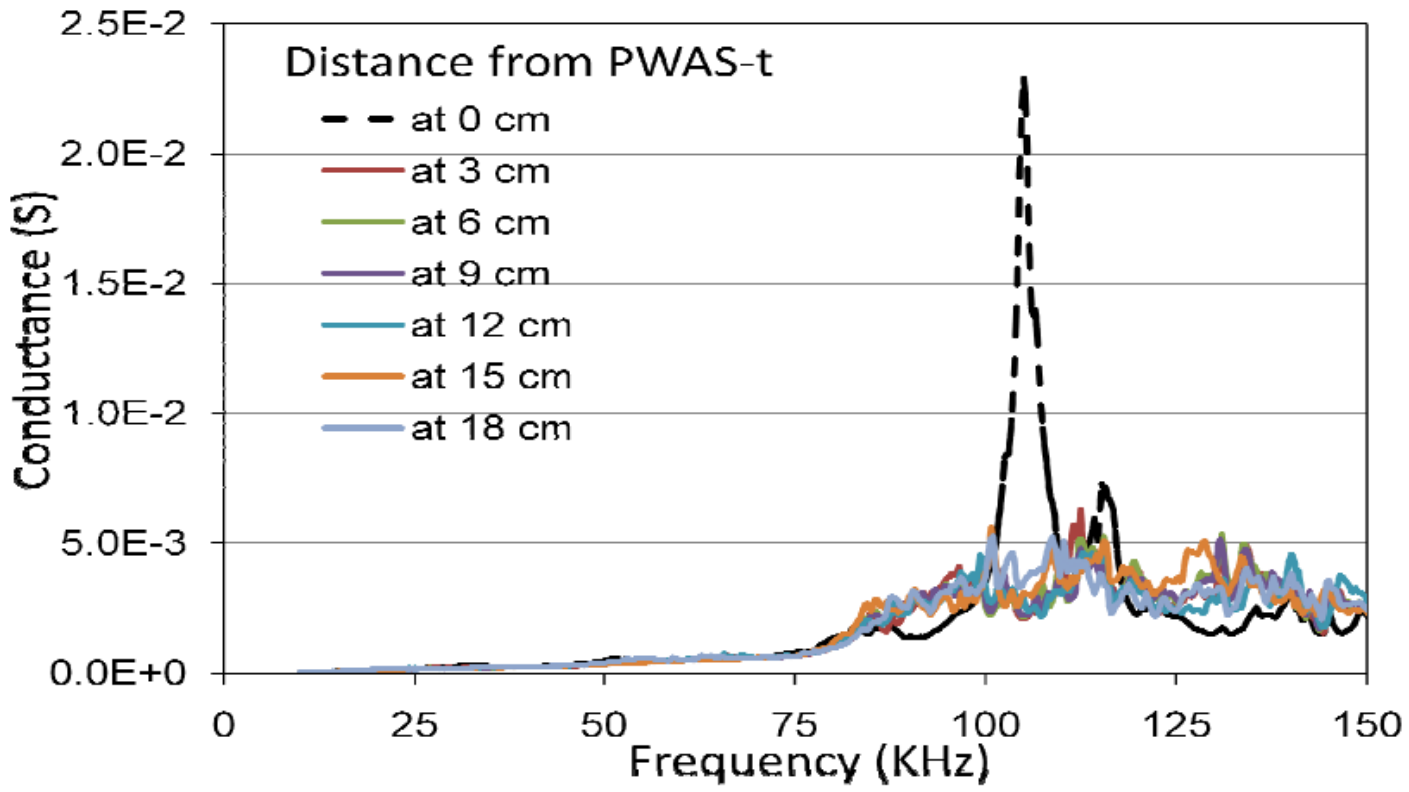

Figure 8. Signatures of crack increments by PWAS-t

Figure 8

Signal Analysis of crack increments (PWAS-t)

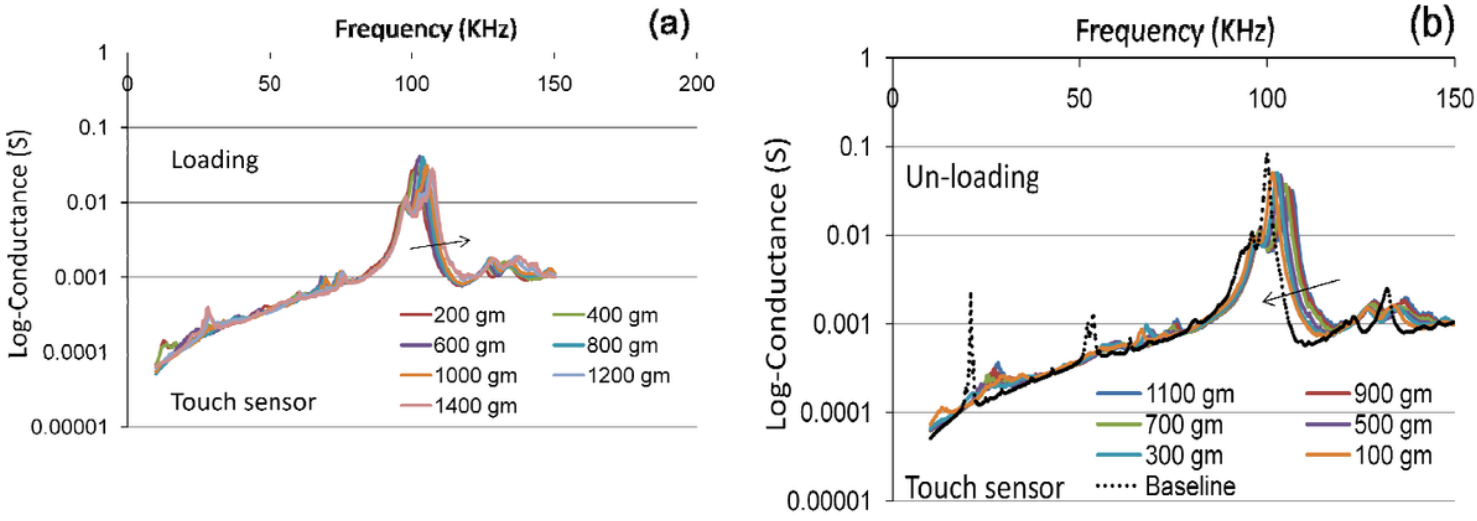

Figure 9. Signatures of load –unload cycle obtained by touch sensor (a) loading steps (b) unloading steps

Figure 9

Signatures (load-unload for touch sensor)

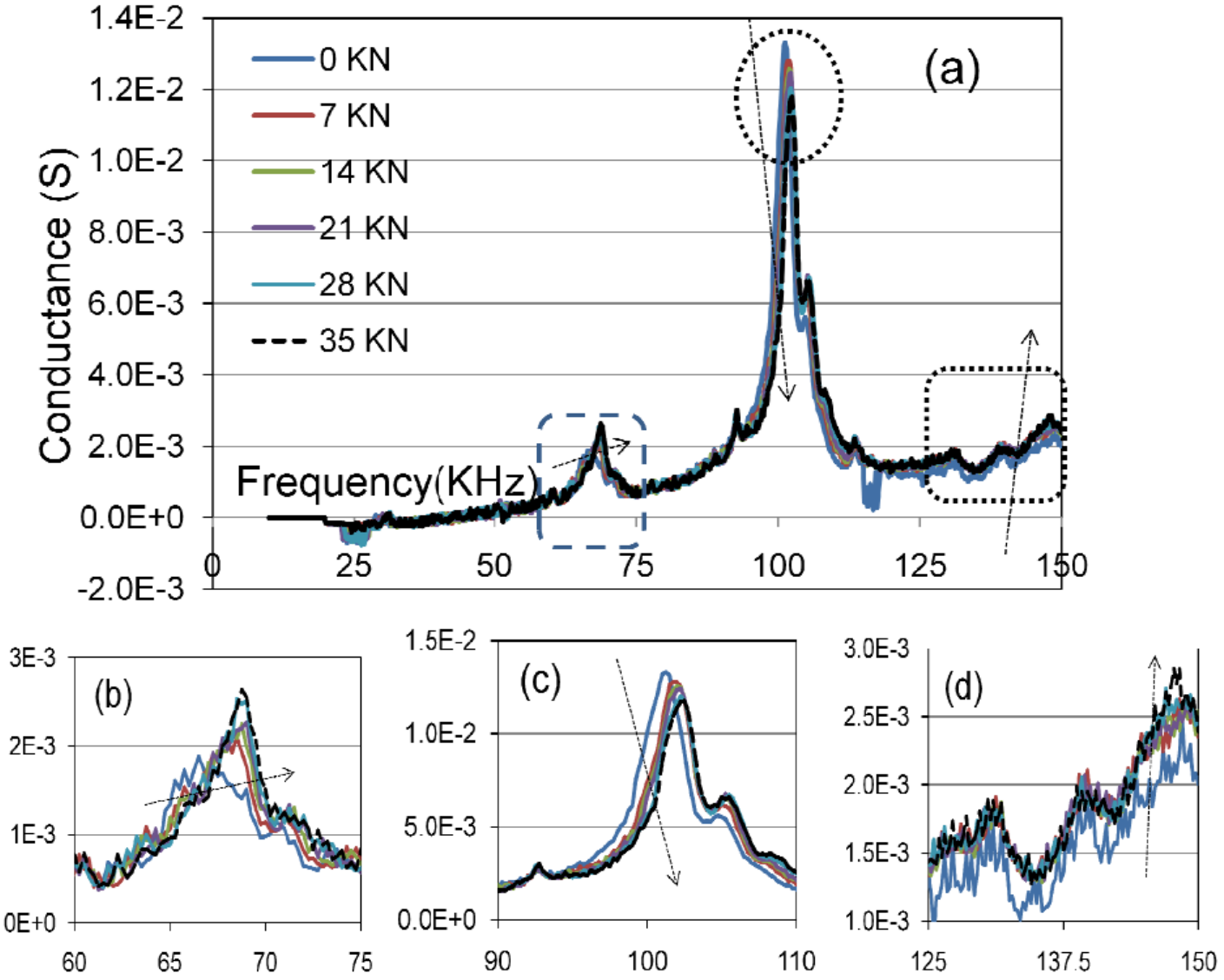

Figure 10. Signatures of tensile test obtained by touch sensor for several incremental steps (a) in wide frequency range (b) rightward shifting of peaks (b) peak magnitude decrement (d) upward shifting of peaks

Figure 10

Signatures (tensile test)

Table 1. Key properties of PZT, Aluminium and magnet

Properties	Values for PZT	Values for A1 6061-T6	Values for AISI 4340 steel	Specific properties of magnet	Values for magnet ($Nd_2Fe_{14}B$) (alloy of neodymium, iron and boron)
Young's modulus N/m^2 x 10^9	63	68.95	186.1	Remanence (B_r),	1.0 - 1.4 Teslas
Poisson's ratio	0.31	0.33	0.3	energy product k.J/m^3	200 - 440
density Kg/m^3	7700	2715	7830	coercive field k. A/m	750–2000
Radius x thickness (mm)	10 x 0.8	-		Radius x thickness (mm)	6 x 4
damping coefficient	0.34	-		Curie temperature (T_c)	310 - 400 °C
piezoelectric constant [m/V] d31 x 10^{-10}	-1.75	-		-	-
relative dielectric constant	1750	-		-	-

Figure 11

Table 1 Key properties

Table 2. RMSD variation for experiments 2 - 4

Cracks at a distance [from Touch sensor] Cm	RMSD (%) [Experiment 2]		Contact Load (gm)	RMSD (%) [Experiment 3]		Axial-tensile load-KN	RMSD (%) [Exp. 4]
	Touch sensor	Bonded sensor		Loading	Unloading		
3	73.781	4.67	200	66.62	80.6	0	-
6	73.74	6.16	400	80	99	7	21.35
9	73.151	15.165	600	104	102.8	14	24.41
12	71.8	33.79	800	100	100.91	21	26.31
15	70.66	35.05	1000	97	98.5	28	30.52
18	66.2	51.81	1200	95	96.44	35	32.75
-	-	-	1400	94.59			

Figure 12

Table 2 RMSD variations (exp 2 - 4)

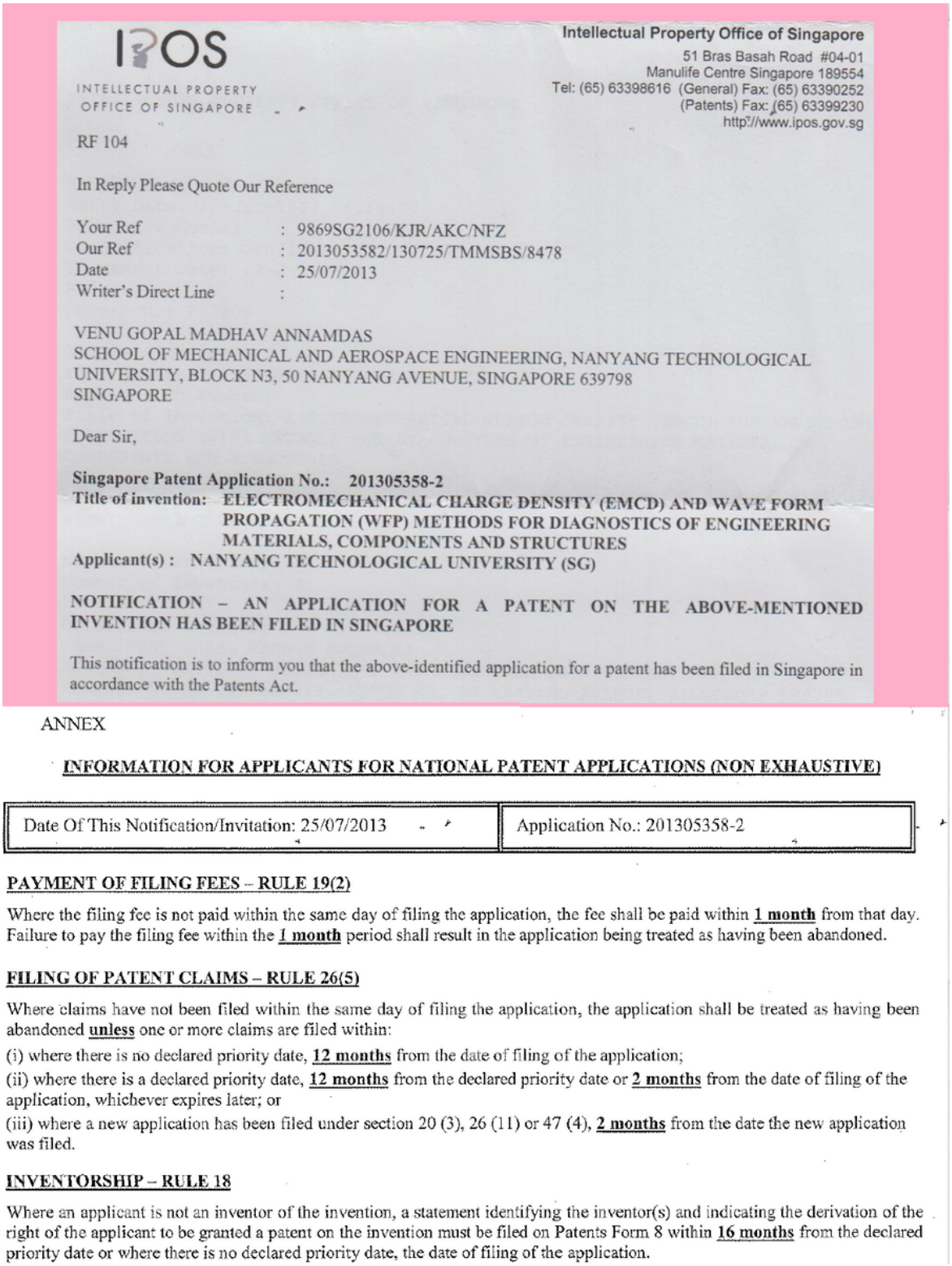

IPOS
INTELLECTUAL PROPERTY OFFICE OF SINGAPORE

Intellectual Property Office of Singapore
51 Bras Basah Road #04-01
Manulife Centre Singapore 189554
Tel: (65) 63398616 (General) Fax: (65) 63390252
(Patents) Fax: (65) 63399230
http://www.ipos.gov.sg

RF 104

In Reply Please Quote Our Reference

Your Ref : 9869SG2106/KJR/AKC/NFZ
Our Ref : 2013053582/130725/TMMSBS/8478
Date : 25/07/2013
Writer's Direct Line :

VENU GOPAL MADHAV ANNAMDAS
SCHOOL OF MECHANICAL AND AEROSPACE ENGINEERING, NANYANG TECHNOLOGICAL UNIVERSITY, BLOCK N3, 50 NANYANG AVENUE, SINGAPORE 639798
SINGAPORE

Dear Sir,

Singapore Patent Application No.: 201305358-2
Title of invention: ELECTROMECHANICAL CHARGE DENSITY (EMCD) AND WAVE FORM PROPAGATION (WFP) METHODS FOR DIAGNOSTICS OF ENGINEERING MATERIALS, COMPONENTS AND STRUCTURES
Applicant(s) : NANYANG TECHNOLOGICAL UNIVERSITY (SG)

NOTIFICATION – AN APPLICATION FOR A PATENT ON THE ABOVE-MENTIONED INVENTION HAS BEEN FILED IN SINGAPORE

This notification is to inform you that the above-identified application for a patent has been filed in Singapore in accordance with the Patents Act.

ANNEX

INFORMATION FOR APPLICANTS FOR NATIONAL PATENT APPLICATIONS (NON EXHAUSTIVE)

Date Of This Notification/Invitation: 25/07/2013	Application No.: 201305358-2

PAYMENT OF FILING FEES – RULE 19(2)

Where the filing fee is not paid within the same day of filing the application, the fee shall be paid within **1 month** from that day. Failure to pay the filing fee within the **1 month** period shall result in the application being treated as having been abandoned.

FILING OF PATENT CLAIMS – RULE 26(5)

Where claims have not been filed within the same day of filing the application, the application shall be treated as having been abandoned **unless** one or more claims are filed within:

(i) where there is no declared priority date, **12 months** from the date of filing of the application;

(ii) where there is a declared priority date, **12 months** from the declared priority date or **2 months** from the date of filing of the application, whichever expires later; or

(iii) where a new application has been filed under section 20 (3), 26 (11) or 47 (4), **2 months** from the date the new application was filed.

INVENTORSHIP – RULE 18

Where an applicant is not an inventor of the invention, a statement identifying the inventor(s) and indicating the derivation of the right of the applicant to be granted a patent on the invention must be filed on Patents Form 8 within **16 months** from the declared priority date or where there is no declared priority date, the date of filing of the application.

Figure 13

Figure 11 Singapore Patent (Protection July 2013 - July 2014)